Chinese Journal of Natural Medicines

A quinolinyl analog of resveratrol improves neuronal damage after ischemic stroke by promoting Parkin-mediated mitophagy

Qingqi Meng, Yan Mi, Libin Xu, Yeshu Liu, Dong Liang, Yongping Wang, Yan Wang, Yueyang Liu, Guoliang Chen, Yue Hou

Citation: Qingqi Meng, Yan Mi, Libin Xu, Yeshu Liu, Dong Liang, Yongping Wang, Yan Wang, Yueyang Liu, Guoliang Chen, Yue Hou, A quinolinyl analog of resveratrol improves neuronal damage after ischemic stroke by promoting Parkin-mediated mitophagy, Chinese Journal of Natural Medicines, 2025, 23(2), 214-224. doi: 10.1016/S1875-5364(25)60825-9.

View online: https://doi.org/10.1016/S1875-5364(25)60825-9

Chinese Journal of Natural Medicines 23 (2025) 214-224

Contents lists available at ScienceDirect

Chinese Journal of Natural Medicines

journal homepage: www.cjnmcpu.com/

Original article

A quinolinyl analog of resveratrol improves neuronal damage after ischemic stroke by promoting Parkin-mediated mitophagy

Qingqi Meng[a], Yan Mi[a], Libin Xu[a], Yeshu Liu[a], Dong Liang[b], Yongping Wang[a], Yan Wang[b], Yueyang Liu[c,*], Guoliang Chen[d,*], Yue Hou[a,*]

[a] *Key Laboratory of Bioresource Research and Development of Liaoning Province, College of Life and Health Sciences, National Frontiers Science Center for Industrial Intelligence and Systems Optimization, Key Laboratory of Data Analytics and Optimization for Smart Industry, Ministry of Education, Northeastern University, Shenyang 110167, China*

[b] *State Key Laboratory for Chemistry and Molecular Engineering of Medicinal Resources, School of Chemistry and Pharmaceutical Sciences, Guangxi Normal University, Guilin 541004, China*

[c] *Shenyang Key Laboratory of Vascular Biology, Science and Research Center, Department of Pharmacology, Shenyang Medical College, Shenyang 110034, China*

[d] *Key Laboratory of Structure-Based Drug Design & Discovery of Ministry of Education, School of Pharmaceutical Engineering, Shenyang Pharmaceutical University, Shenyang 110016, China*

ARTICLE INFO

Article history:
Received 14 March 2024
Revised 4 May 2024
Accepted 25 June 2024
Available online 20 February 2025

Keywords:
(*E*)-4-(3,5-dimethoxystyryl) quinoline
Resveratrol
Ischemic stroke
Mitophagy
Parkin

ABSTRACT

Ischemic stroke (IS) is a prevalent neurological disorder often resulting in significant disability or mortality. Resveratrol, extracted from *Polygonum cuspidatum* Sieb. et Zucc. (commonly known as Japanese knotweed), has been recognized for its potent neuroprotective properties. However, the neuroprotective efficacy of its derivative, (*E*)-4-(3,5-dimethoxystyryl) quinoline (RV02), against ischemic stroke remains inadequately explored. This study aimed to evaluate the protective effects of RV02 on neuronal ischemia-reperfusion injury both *in vitro* and *in vivo*. The research utilized an animal model of middle cerebral artery occlusion/reperfusion and SH-SY5Y cells subjected to oxygen-glucose deprivation and reperfusion to simulate ischemic conditions. The findings demonstrate that RV02 attenuates neuronal mitochondrial damage and scavenges reactive oxygen species (ROS) through mitophagy activation. Furthermore, Parkin knockdown was found to abolish RV02's ability to activate mitophagy and neuroprotection *in vitro*. These results suggest that RV02 shows promise as a neuroprotective agent, with the activation of Parkin-mediated mitophagy potentially serving as the primary mechanism underlying its neuroprotective effects.

1. Introduction

Stroke remains a leading cause of mortality worldwide [1, 2], with ischemic stroke (IS) constituting the most prevalent form [3]. IS occurs due to inadequate blood flow or occlusion of cerebral blood vessels [1, 4, 5]. Current clinical guidelines advocate for reperfusion therapies, including intravenous thrombolysis and endovascular thrombectomy, as the most efficacious interventions for IS [6]. Nowadays, we have entered the era of highly effective reperfusion, where reperfusion therapies restore blood flow to affected areas of the brain along with potentially more severe neurological damage or dysfunction, the phenomenon known as cerebral ischemia/reperfusion injury (CIRI) [7, 8]. Studies indicate that the administration of neuroprotective agents during and after reperfusion can mitigate CIRI and reduce neuronal mortality [9]. Despite these advancements, clinically effective neuroprotectants remain elusive [10]. Consequently, there is an urgent need to identify and develop pharmacological interventions that can improve outcomes for stroke patients.

Mitophagy is a critical process that preserves mitochondrial integrity and function, influencing cellular fate and serving as the primary mechanism for mitochondrial renewal. During reperfusion and oxygen restoration, mitochondria generate excessive reactive oxygen species (ROS). ROS accumulation can trigger the opening of the mitochondrial transition pore (mPTP), leading to mitochondrial membrane potential (ΔΨm) impairment and the release of pro-apoptotic factors such as cytochrome C (Cyt C). This cascade activates the mitochondria-dependent apoptosis pathway, exacerbating tissue damage [11-16]. Mitophagy, mitigates neuronal death by reducing ROS production and eliminating surplus mitochondria. Research has identified Parkin, an RING-between-RING (RBR) E3 ubiquitin-protein ligase, as a crucial regulator of mitophagy in the central nervous system. Damaged mitochondria activate Parkin [17], which subsequently ubiquitinates various mitochondrial proteins. These damaged mitochondria bind to lysosomes through sequestosome-1 (p62) and microtubule-associated protein 1 light chain 3B (LC3B), resulting in their degradation [18, 19]. Additionally, Parkin has been demonstrated to influence the function and stability of excitatory glutamatergic synapses [13, 20, 21]. Consequently, targeting Parkin-mediated mitophagy may represent a promising approach for ischemic stroke treatment.

* Corresponding author.
E-mail addresses: yueyangliu1989@163.com (Y. Liu); chenguoliang@syphu.edu.cn (G. Chen); houyue@mail.neu.edu.cn (Y. Hou)

https://doi.org/10.1016/S1875-5364(25)60825-9

(*E*)-4-(3,5-dimethoxystyryl) quinoline (RV02) is a resveratrol (RES) derivative featuring a structural modification that substitutes RES's 3,5-dihydroxyl groups with 3,5-dimethoxy groups and its phenolic group with a quinolinyl moiety. While RES offers various pharmacological benefits, including neuroprotection, its clinical application is limited by low oral bioavailability and instability [22-25]. Chemical modifications, such as methylation of RES's hydroxyl groups, have been demonstrated to enhance its stability and bioavailability, providing protection against phase II metabolic processes like glucuronidation and sulfation [26]. These RES derivatives have exhibited superior antiplatelet aggregation properties [27]. RV02 has demonstrated greater efficacy than RES in reducing neuropathic inflammation and repairing DNA damage, both of which are closely associated with stroke pathogenesis [28, 29]. Furthermore, quinoline derivatives are known for their anti-apoptotic properties [30]. Considering these characteristics, we hypothesize that RV02 may be a potential compound for the treatment of IS. However, there is currently a lack of experimental evidence confirming RV02's efficacy in improving IS outcomes.

This study investigates the potential therapeutic effects of RV02 on IS, with a specific focus on neuroprotection. The findings indicate that RV02 demonstrates the capacity to mitigate neuronal damage following CIRI through multiple mechanisms: inhibiting neuronal apoptosis, attenuating oxidative stress, and enhancing mitochondrial function. Further mechanistic exploration reveals that RV02's neuroprotective effects are associated with the augmentation of Parkin-mediated mitophagy, which serves to counteract the detrimental cycle of oxidative stress and mitochondrial dysfunction.

2. Materials and methods

2.1. Synthesis of RV02

The structure of RV02 is illustrated in Fig. 1A. The compound RV02 was synthesized using a previously described method [31, 32]. In brief, 3,5-dimethoxybenzyl chloride was dissolved in triethyl phosphite and refluxed for 4 h to obtain an oil residue. Subsequently, *N*,*N*-dimethylformamide (DMF) and EtONa were added to the oil residue. After 5 min of stirring, 4-quinolinecarbaldehyde was introduced. The mixture was stirred for an additional 4 h before being poured into water. The resulting product, a yellow solid, was recrystallized in alcohol (Scheme 1).

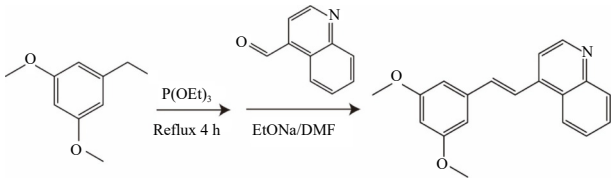

Scheme 1 The synthetic route of RV02.

2.2. MCAO/R model establishment

Male Sprague Dawley rats (Liaoning Changsheng Biotechnology Co., Ltd.), weighing 220–250 g, were utilized for animal experiments. The study adhered to the regulations of the Experimental Animal Administration of the State Science and Technology Commission of China. Animal studies received approval from the Animal and Medical Ethics Committee of Northeastern University (Registration No. NEU-EC-2022A030S). The rats were randomly assigned to the sham-operated group, MCAO/R group, groups receiving various doses of RV02 (7, 14, and 28 mg·kg^{-1}), and the RES group.

The MCAO/R model was established according to previously described methods [33, 34]. In brief, rats were anesthetized with a 2.5% tribromoethanol intraperitoneal injection. Subsequently, a neck incision was made to isolate the right carotid arteries, including the common carotid (CCA) and external and internal carotid arteries (ECA, ICA). A nylon suture with a coated tip was then inserted from the CCA into the ICA for 1.5–2.0 cm to occlude the middle cerebral artery (MCA). In the sham group, only CCA, ECA, and ICA were separated. Following the surgery, the incision was sutured and disinfected. A temperature-controlled heating pad was used to maintain the animal's body temperature throughout the procedure. After 2 h, the thread was removed. Rats were immediately administered 1.0% carboxymethylcellulose (CMC-Na), RV02 (7, 14, and 28 mg·kg^{-1} suspended in 1.0% CMC-NA), or RES (28 mg·kg^{-1} suspended in 1.0% CMC-NA) *via* intragastric administration.

2.3. Neurological deficits assessment

The neurological deficits were evaluated using the Longa scale [35] and assessed at 0 and 24 h following MCAO/R. The scale has a maximum score of four points. Trained examiners conducted the neurobehavioral tests, adhering to the double-blind protocol.

2.4. MRI studies

The rats were anesthetized with 2.5% tribromoethanol and subsequently positioned within the magnet using an animal holder/MRI probe apparatus, ensuring secure immobilization of the animal's head within the imaging coil. All MRI measurements were conducted using the M5 Compact MRI System (Aspect Imaging Ltd., Israel). T2-weighted magnetic resonance imaging was performed with the following parameters: field of view = 0.2 cm × 0.2 cm, number of slices = 10, slice thickness = 2 mm, slice orientation = Axial, repetition time/echo time = 3000/71.15 ms.

2.5. Brain water content and cerebral infarct volume assessment

The rats were anesthetized using 2.5% tribromoethanol and subsequently euthanized by decapitation. Following the complete removal of surrounding tissues, the brain was immediately weighed. The brain slices were then allowed to dry naturally before being weighed again. To determine the brain water content, the following equation was applied: (wet weight of brain − dry weight of brain)/wet weight of brain × 100%.

Following MCAO/R, the infarct volume was assessed using TTC staining. The procedure involved weighing the brain and immediately freezing it at −20 °C for 15 min. The brain was then sectioned into five equal slices and incubated in a 2% TTC solution at 37 °C for 25 min. Image J software was employed to analyze the infarct areas on each slice. The infarct volume was calculated using the formula [(infarct size × 2 mm)/2] × ipsilateral hemisphere volume × 100%.

2.6. Immunofluorescence

Brain tissues were fixed in 4% paraformaldehyde (PFA) at 4 °C for 24 h, followed by dehydration in 30% and 20% sucrose solutions. Frozen sections were prepared for immunofluorescence analysis. After antigen retrieval with 6% citrate buffer, brain slices were incubated for one h with 5% goat serum. Immunostaining was subsequently performed with overnight incubation of primary antibody (1∶1000 anti-NeuN, Abcam, Cambridge, MA, USA, ab177487) followed by 90-min incubation with secondary antibody (1∶500 anti-rabbit IgG, Absin, Shanghai, China). DAPI (Beyotime Biotechnology, P0131) was utilized for

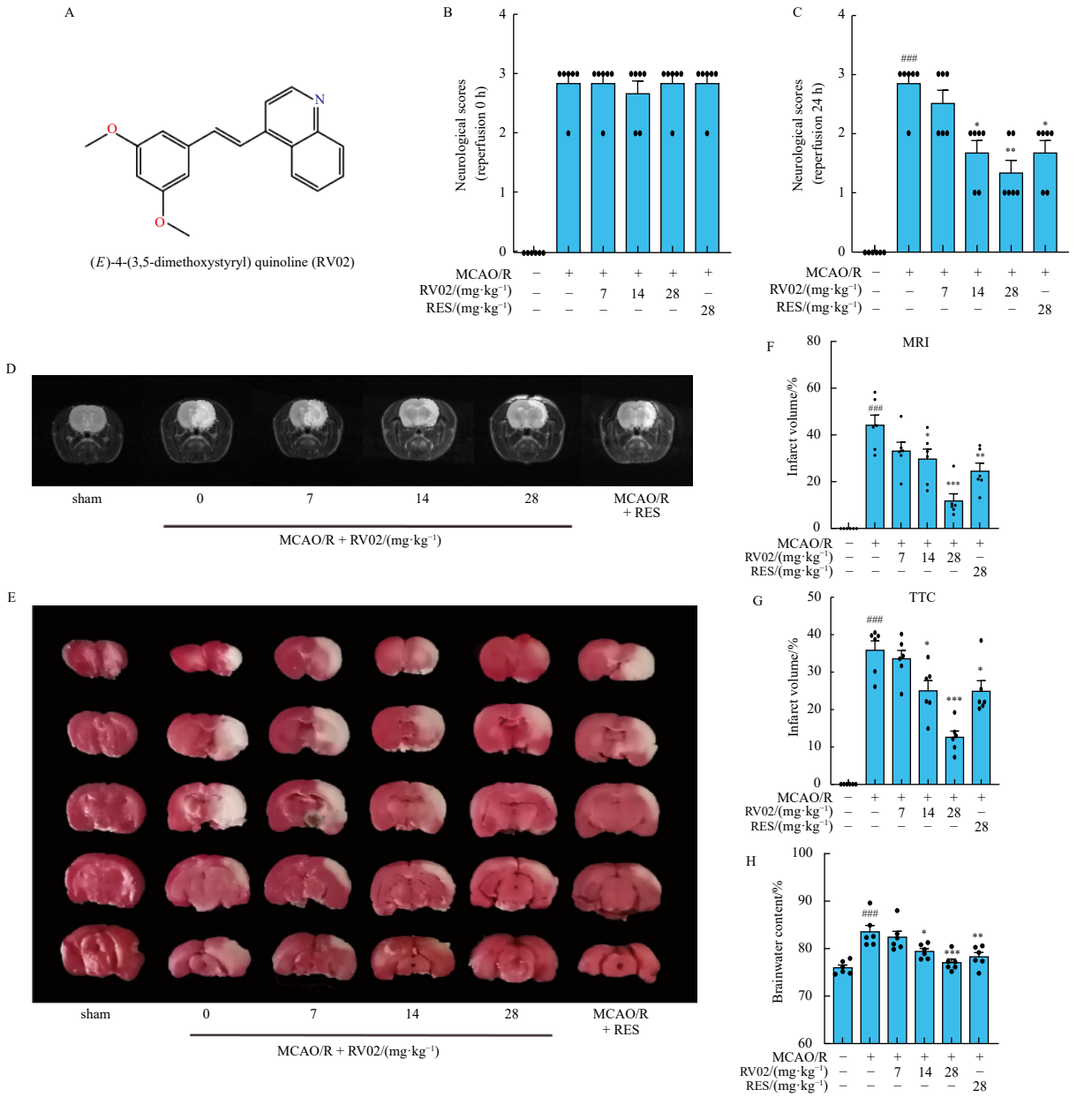

Fig. 1 RV02 mitigated neurological deficits following middle cerebral artery occlusion/reperfusion (MCAO/R) surgery. (A) Structure of RV02. (B and C) Neurological scores were assessed at 0 and 24 h after MCAO/R surgery (n = 6). (D) Evaluation of the ischemic lesion volume with T_2WIs. (E) Cerebral infarct volumes were measured by TTC staining. (F and G) Quantification of cerebral infarct volume detected by magnetic resonance imaging (MRI) and TTC methods, respectively (n = 6). (H) Brain water content was determined (n = 6). Data are presented as mean ± SEM. Statistical analysis: a one-way analysis of variance (ANOVA) followed by Tukey's test. $^{###}P < 0.001$ *vs* control; $^{*}P < 0.05$, $^{**}P < 0.01$, $^{***}P < 0.001$ *vs* MCAO/R group. RES: resveratrol (28 mg·kg^{-1}).

nuclear staining.

2.7. Cell culture and establishment of cell models

Primary neurons were isolated from the brains of newborn mice. The brain tissue was swiftly extracted, and the meninges were meticulously removed. Subsequently, the tissue was immersed in Dulbecco's modified eagle medium (DMEM)/F12 (Gibco, C11330500BT) and subjected to digestion using 0.25% trypsin. Following digestion, the trypsin was carefully aspirated using a pipette, and DMEM/F12 (Gibco, C11330500BT) containing fetal bovine serum (FBS) and penicillin-streptomycin (PS) was introduced to halt the digestion process. The resulting cell suspension was seeded onto a culture plate containing neurobasal medium (Thermo Fisher Scientific, 21103049) supplemented with B27 (Thermo Fisher Scientific, 17504044). The culture plate was then incubated at 37 °C in an atmosphere containing 5% CO_2.

Neuroblastoma SH-SY5Y cells were cultured in DMEM (Gibco, Waltham, MA, USA, C11965500BT) supplemented with 10% FBS and 1% penicillin-streptomycin. To establish the oxygen-glucose deprivation/reperfusion (OGD/R) model, cells were incubated in glucose-free medium at 95% CO_2–5 % N_2 for 4 h. Subsequently, the medium was replaced with either normal DMEM or DMEM containing RV02 (1, 3, 10 μmol·L^{-1}) or RES (10 μmol·L^{-1}) for 24 h.

2.8. Cell viability

Following a 24-h treatment of primary neurons and SH-SY5Y cells with or without OGD/R, 10 μL of MTT was added to each well. The cells were then incubated for 4 h, after which 150 μL of dimethyl sulfoxide (DMSO) was added. Cell viability was subsequently measured at 490 nm using a microplate reader.

2.9. Western blotting analysis

Radio immunoprecipitation assay (RIPA) lysis buffer

(Beyotime Biotechnology, P0013B) was used to extract total protein, while a mitochondrial extract kit (Beyotime Biotechnology, C3606, C3601) was employed to isolate mitochondrial protein. Protein lysates (40 μg) were separated using sodium dodecyl sulfate-polyacrylamide gel electrophoresis (SDS-PAGE) (12% and 15%) and subsequently transferred to a PVDF membrane. The immune blots were then blocked with 5% skimmed milk. Membranes were incubated overnight at 4 °C with primary antibodies against Bcl-2-associated X protein (Bax) (1∶1000, CST, Danvers, MA, USA, 14796S), Bcl-2 (1∶1000, Abcam, ab182858), Cyt C (1∶1000, CST, Danvers, MA, USA, 4280), p62 (1∶1000, CST, 39749), Parkin (1∶500, Abcam, ab77924), LC3 (1∶1000, Proteintech, 14600-1-AP), TOMM20 (1∶1000, Abcam, ab186734), cytochrome c oxidase subunit IV (COX IV) (1∶1000, CST, 11967), or *β*-actin (1∶10 000, Proteintech, Chicago, IL, USA, 66009-1-Ig). Secondary antibodies against rabbit (CST, 7074) and mouse IgG (Proteintech, PA1-28555) were incubated at room temperature for 1 h.

2.10. Transferase dUTP nick end labeling (TUNEL) staining

The terminal deoxynucleotidyl TUNEL assay was performed to evaluate apoptosis in SH-SY5Y cells using a commercial kit (Beyotime Biotechnology, C1089) following 24 h of OGD/R treatment. Cells were incubated with 50 μL of TUNEL solution at 37 °C for 30 min. Subsequently, DAPI was applied for 10 min to stain the nuclei.

2.11. Determined by dichlorodihydrofluorescein diacetate assay (DCFH-DA), dihydroethidium (DHE), and MitoSOX-red staining

ROS levels in *in vivo* brain tissue and oxidative stress model cells were quantified using the DCFH-DA staining method (Beyotime Biotechnology, S0033M). For tissue samples, approximately 0.02 g of tissue was homogenized in 180 μL phosphate-buffered saline (PBS). Following centrifugation, 5 μL of supernatant and 195 μL of DCFH-DA (10 μmol·L^{-1}) were added to 96-well plates. The cells were incubated at room temperature for 30 min with DCFH-DA (10 μmol·L^{-1}). Fluorescent signal intensity was measured at an emission wavelength of 500 nm and an excitation wavelength of 525 nm. ROS production in OGD/R model cells was detected using DHE (Beyotime Biotechnology, S0063). Mitochondrial ROS levels were evaluated using MitoSOX-red (Thermo Fisher Scientific, M36008). Similar staining protocols were employed for both DCFH-DA and DHE. After staining, the cells were visualized using fluorescence microscopy.

2.12. Detection of superoxide dismutase (SOD), malondialdehyde (MDA), glutathione (GSH), and H_2O_2

Following OGD/R, the cells were collected and centrifuged. Subsequently, the SOD activity and the concentrations of MDA, reduced GSH, and H_2O_2 were assessed. Commercial assay kits from Beyotime Biotechnology (Beijing, China) were utilized to quantify SOD activity (S0101S), MDA levels (S0131M), GSH levels (S0053), and H_2O_2 levels (S0038) in accordance with the manufacturer's protocols.

2.13. JC-1 staining

The cellular mitochondrial membrane potential (MMP) was evaluated using JC-1 (Beyotime Biotechnology, C2003S), a dual-emission membrane potential-sensitive dye. Following 24 h of OGD/R treatment, cells were washed with PBS before the addition of JC-1. After 30 min incubation at 37 °C, measurements were taken at 490 nm/530 nm (JC-1 aggregates) and 525 nm/590 nm (JC-1 monomer), or cells were observed under a fluorescence microscope. For brain tissues, mitochondria were extracted using a mitochondrial extract kit (Beyotime Biotechnology, C3606). The extracted mitochondria were then combined with the JC-1 solution and measured using a microplate reader.

2.14. ATP content assessment

Intracellular ATP quantification was performed using a commercial kit (Beyotime Biotechnology, S0026). Briefly, tissue sample homogenates and cell lysates were centrifuged to obtain supernatants. Following the manufacturer's protocol, 100 μL of ATP detection solution was added to each well of a 96-well plate. Subsequently, 20 μL of sample supernatant was introduced and rapidly mixed. The luminescence was then measured using a luminometer.

2.15. Fluorescent imaging of LC3-GFP and Mito-Tracker Red

SH-SY5Y cells were transfected with a plasmid containing the LC3-GFP reporter gene. The cells in each experimental group underwent 48 h of infection, followed by OGD/R treatment, with the exception of the control group. After 24 h of OGD/R exposure, mitochondrial staining was performed using Mito-Tracker Red (Beyotime Biotechnology, C1035), while Hoechst 33342 (Beyotime Biotechnology, C1025) was employed for nuclear staining.

2.16. siRNA knockdown

The Parkin siRNA (sense: 5′-UUCGCAGGUGACUUUCCUCUGGGUC-3′, antisense: 5′-UGACCAGAGGAAAGUCACCUGCGAA-3′) was synthesized by Suzhou GenePharma Co., Ltd. (Suzhou, China). The siRNA was introduced into SH-SY5Y cells using LipoRNAi (Beyotime Biotechnology, C0535) according to the manufacturer's instructions. Briefly, the siRNAs and LipoRNAi transfection reagent were combined in DMEM (without FBS) for 20 min. Four hours after transfection, the medium was replaced with DMEM containing FBS. Subsequently, 48 h later, a fluorescent GFP-tagged LC3 plasmid was utilized for cell transfection. The transfection efficiency was evaluated by western blotting.

2.17. Statistical analysis

Data variance across experimental groups was analyzed using ANOVA, followed by Tukey's test or Dunnett's T3 test. Statistical analysis was performed using SPSS 25.0 software, while bar graphs were generated using GraphPad Prism 7.0. All data are expressed as mean ± standard error of the mean (SEM). Statistical significance was denoted as $^{\#}P < 0.05$, $^{\#\#}P < 0.01$, $^{\#\#\#}P < 0.001$ *vs* control; $^{*}P < 0.05$, $^{**}P < 0.01$, $^{***}P < 0.001$ *vs* MCAO/R group or OGD/R group.

3. Results

3.1. RV02 attenuated neurological deficits after ischemia/reperfusion

Laser speckle blood flow measurements clearly demonstrated that regional cerebral blood flow (rCBF) decreased following MCAO surgery in mice, and RV02 (40 mg·kg^{-1}) significantly improved rCBF 24 h post-reperfusion (Supplementary Fig. S1). Based on the conversion principle, RV02 (28 mg·kg^{-1}) was selected as the maximum dose for animal experiments. To investigate RV02's potential protective effects against CIRI, the MCAO/R model was utilized. Neurological scores at 0 and 24 h post-reperfusion, ischemic lesion size, brain infarct volume, and brain water content were assessed to evaluate brain damage. The

results revealed that RV02, at dosages of 14 and 28 mg·kg^{-1}, significantly reduced neurological scores (Figs. 1B and 1C). IS size was estimated using *in vivo* MRI. T2-weighted images were captured 24 h after blood flow restoration. RV02-treated rats exhibited smaller lesion sizes, indicated by areas of high intensity, compared to the control group that underwent ischemia-reperfusion (Figs. 1D and 1E). The results of cerebral infarct area (Figs. 1F and 1G) and brain water content (Fig. 1H) aligned with the findings of *in vivo* detection of ischemic lesions. At doses of 14 and 28 mg·kg^{-1}, RV02 significantly reduced brain water content and cerebral infarct area in rats compared to the MCAO/R group. Moreover, RV02 administered at a dose of 28 mg·kg^{-1} demonstrated superior efficacy to RES. These findings indicate that RV02 can markedly ameliorate brain injury following ischemia-reperfusion.

3.2. RV02 mitigated ischemia/reperfusion-induced neuronal death

Neuronal death is the primary cause of neurological dysfunction. For example, previous research indicates that cognitive impairment emerges after 8 weeks of cerebral hypoperfusion in rats and correlates with the onset of neuronal damage in the brain [36]. To investigate the neuroprotective effects of RV02, we initially conducted immunofluorescence staining to quantify mature neurons in the brains of MCAO/R rats. Fig. 2A demonstrated that RV02 treatment alleviated neuronal defects in the ipsilateral hemisphere of the infarct area. The regional pattern of immunofluorescence detection of the ischemic penumbra was depicted in

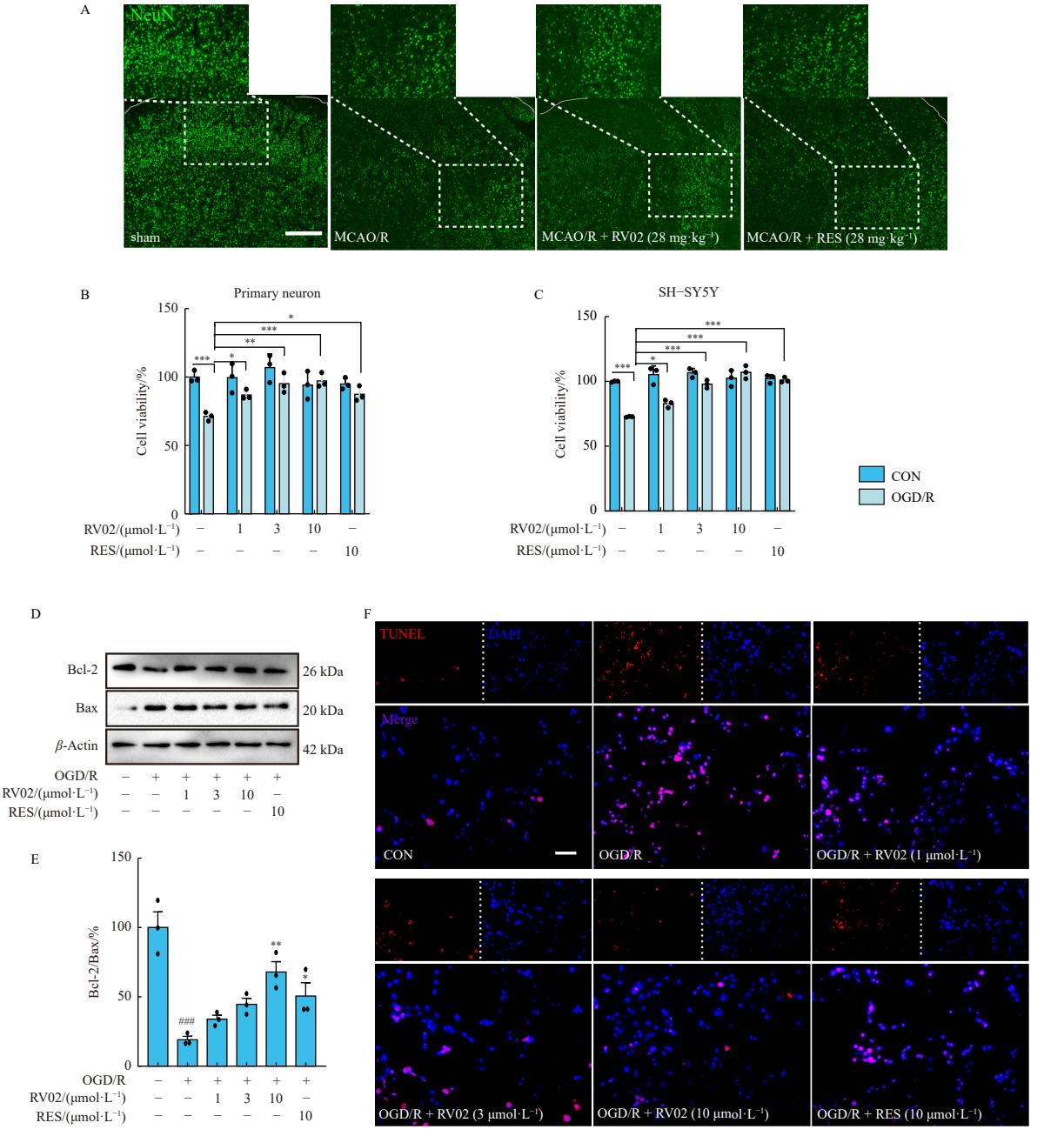

Fig. 2 RV02 inhibited neuronal death induced by ischemia/reperfusion. (A) Representative immunofluorescence images (scale bar: 200 μm) illustrating the number of NeuN + cells in the cortex of the infarcted area following MCAO/R surgery. (B) Primary neuron viability with or without OGD/R and RV02 or RES treatment (n = 3). (C) SH-SY5Y cell viability with or without OGD/R and RV02 or RES treatment (n = 3). (D and E) The ratio of Bcl-2/Bax was determined by Western blot analysis (n = 3). (F) Representative immunofluorescence images (scale bar: 200 μm) depicting the extent of TUNEL-positive cells after OGD/R treatment. Data are presented as mean ± SEM. Statistical analysis: one-way ANOVA followed by Tukey's test. $^{###}P < 0.001$ *vs* control; $^{*}P < 0.05$, $^{**}P < 0.01$, $^{***}P < 0.001$ *vs* MCAO/R group or OGD/R group. RES: resveratrol (28 mg·kg^{-1}, 10 μmol·L^{-1}).

Supplementary Fig. S2. Subsequently, we performed cell viability assays to assess the potential cytotoxicity of RV02 in primary-cultured neuronal cells. We noted that RV02 treatment did not affect neuron viability at concentrations of 1, 3, and 10 μmol·L^{-1} (Fig. 2B). Consequently, we further examined the potential neuroprotective benefits of RV02 on primary neuron cells exposed to OGD/R injury. At concentrations of 1, 3, and 10 μmol·L^{-1}, RV02 significantly enhanced neuron viability (Fig. 2B). Similar effects were also observed in SH-SY5Y cells (Fig. 2C). Western blotting results revealed that OGD/R injury significantly reduced the ratio of the anti-apoptotic protein Bcl-2 to the pro-apoptotic protein Bax; however, RV02 treatment reversed these effects (Figs. 2D and 2E). Correspondingly, TUNEL staining demonstrated that RV02 decreased the number of TUNEL-positive cells in SH-SY5Y cells following OGD/R treatment (Fig. 2F). These findings suggest that RV02 can mitigate neuronal apoptosis induced by ischemia-reperfusion.

3.3. RV02 ameliorates neuronal oxidative stress following ischemia-reperfusion

Reperfusion following cerebral ischemia initiates a complex cascade of pathological events, resulting in neuronal damage [37]. The excessive production of ROS exacerbates cell death and brain damage post-CIRI [29, 38]. Our findings demonstrate that RV02 diminished the co-localization levels of DHE and neuronal nuclei (NEUN), as well as intracellular ROS content following MCAO/R (Figs. 3A and 3B). Additionally, RV02 reduced the number of DHE-positive and DCFH-DA-positive cells, along with intracellular ROS levels after OGD/R (Figs. 3C–3E). OGD/R treatment significantly decreased GSH levels and SOD enzyme activity while increasing MDA and H_2O_2 levels in SH-SY5Y cells. Conversely, RV02 treatment enhanced GSH levels and SOD enzyme activity while reducing MDA and H_2O_2 levels compared to OGD/R-treated cells (Figs. 3F–3I).

3.4. RV02 ameliorates mitochondrial dysfunction

Enhancement of mitochondrial function and quality control can significantly improve neuronal recovery [39]. Mitochondrial dysfunction is a major contributor to cell death and a significant source of ROS [11]. To evaluate the effect of RV02 on mitochondrial damage following MCAO/R, we assessed MMP using JC-1 staining. RV02 mitigated the MCAO/R-induced decrease in MMP (Fig. 4A). The *in vitro* results from OGD/R-treated SH-SY5Y cells corroborated the *in vivo* findings (Fig. 4B). Subsequently, we measured ATP levels, a critical indicator of mitochondrial injury. We found that MCAO/R reduced total ATP, which was prevented by RV02 treatment (Fig. 4C). Consistently, we observed similar ATP restoration after RV02 treatment in OGD/R-treated SH-SY5Y cells (Fig. 4D). Mitochondrial damage can induce the translocation of Cyt C from mitochondria to the cytoplasm, thereby initiating ap-

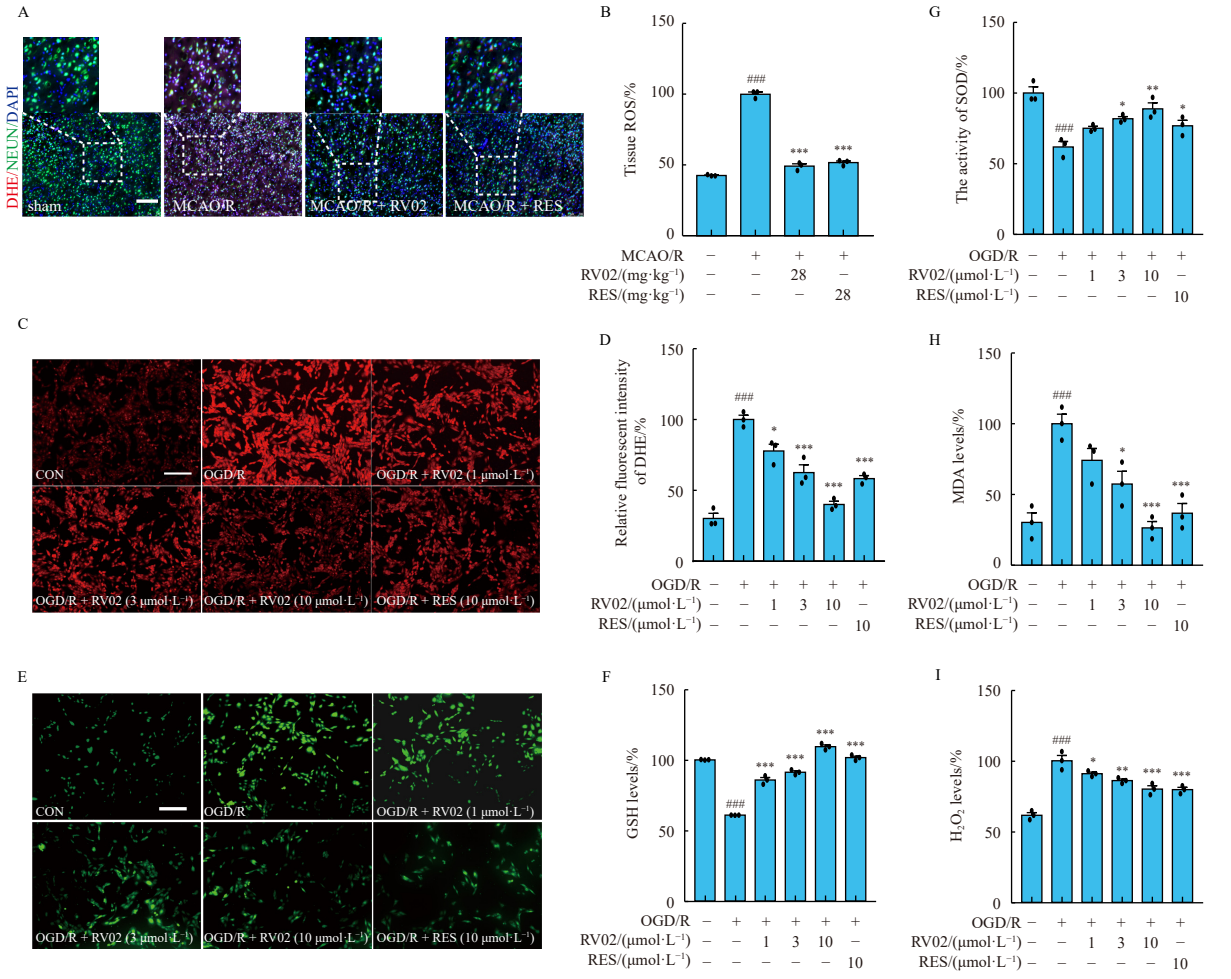

Fig. 3 RV02 inhibits oxidative stress induced by ischemia-reperfusion. (A) Co-localization of DHE and NEUN in the cortex of cerebral ischemic areas detected by immunofluorescence, red: DHE, green: NEUN, blue: DAPI. (B) The release of ROS in the cerebral cortex of MCAO/R rats was determined with a DCFH-DA probe (n = 3). (C and D) The relative fluorescence of DHE in SH-SY5Y cells after OGD/R treatment (n = 3, scale bar = 200 μm). (E) Immunofluorescence detection of DCFH-DA fluorescence intensity in SH-SY5Y cells after OGD/R treatment. (F–I) The levels of MDA, GSH, H_2O_2 and the activity of SOD in SH-SY5Y cells after OGD/R treatment (n = 3). Data are expressed as mean ± SEM. Statistical analysis: one-way ANOVA followed by Tukey's test. $^{###}P < 0.001$ *vs* control; $^{*}P < 0.05$, $^{**}P < 0.01$, $^{***}P < 0.001$ *vs* MCAO/R group or OGD/R group. RES: resveratrol (28 mg·kg^{-1}, 10 μmol·L^{-1}).

optotic cell death. RV02 increased mitochondrial Cyt C levels while decreasing cytoplasmic Cyt C levels in SH-SY5Y cells following OGD/R (Figs. 4E and 4F).

3.5. RV02 enhanced mitophagy after ischemia/reperfusion

Damaged mitochondria and accumulated ROS can initiate mitophagy to mitigate intracellular damage [40]. Therefore, we subsequently examined the effect of RV02 on mitophagy and the expression levels of mitochondrial markers COX IV and TOMM20. RV02 increased the expression of Parkin and LC3-II while reversing the expression of p62 and COX IV following MCAO/R treatment (Figs. 5A–5E). After OGD/R treatment, RV02 reduced the expression of Parkin in the cytoplasm and elevated its expression in the mitochondria (Figs. 5F–5H). Similarly, RV02 enhanced the expression of Parkin and LC3-II but reversed the expression of p62 and COX IV following OGD/R treatment (Figs. 5I–5M). Additionally, RV02 facilitated the mitochondrial translocation of Parkin (Supplementary Fig. S1). Moreover, RV02 increased the co-localization of LC3 and mitochondria after OGD/R (Fig. 5N). These findings indicate that RV02 can enhance mitophagy.

3.6. RV02 disrupted the cyclical pattern of mitochondrial damage and oxidative stress by enhancing Parkin-mediated mitophagy in the ischemia/reperfusion model

To investigate whether RV02 disrupts the detrimental cycle of mitochondrial damage and oxidative stress by promoting mitophagy, we employed a mitophagy inhibitor (Mdivi-1) and an autophagy inhibitor (3-MA) to block mitophagy and autophagy, respectively. Figs. 6A–6C demonstrate that mitophagy, we used a Mdivi-1 and 3-MA counteracted RV02's impact on COX IV and TOMM20 levels. Mdivi-1 and 3-MA reversed RV02's therapeutic effects on intercellular ROS, mitochondrial ROS, and MMP (Figs. 6D–6F). As Parkin mediates mitophagy activation, we examined Parkin's involvement in RV02-induced mitophagy by knockdown experiments (Supplementary Fig. S3). MTT results revealed that Parkin knockdown following RV02 treatment does not alter SH-SY5Y cell activity caused by OGD/R (Fig. 6G). Parkin knockdown reversed RV02-induced mitophagy (Fig. 6H). This observation suggests that RV02's ability to disrupt the detrimental cycle of mitochondrial damage and oxidative stress may depend on its regulation of Parkin-mediated mitophagy.

4. Discussion

The investigation corroborated the neuroprotective attributes of RV02, a quinolinyl analog of RES, in the context of ischemic stroke. This protective effect may be attributed to RV02's ability to restore cerebral blood flow. Furthermore, mitochondria play a pivotal role in brain energy metabolism, and targeting these organelles has been demonstrated to modulate mechanisms associated with post-CIRI conditions such as oxidative stress and inflammation. The research elucidated that RV02's protect-

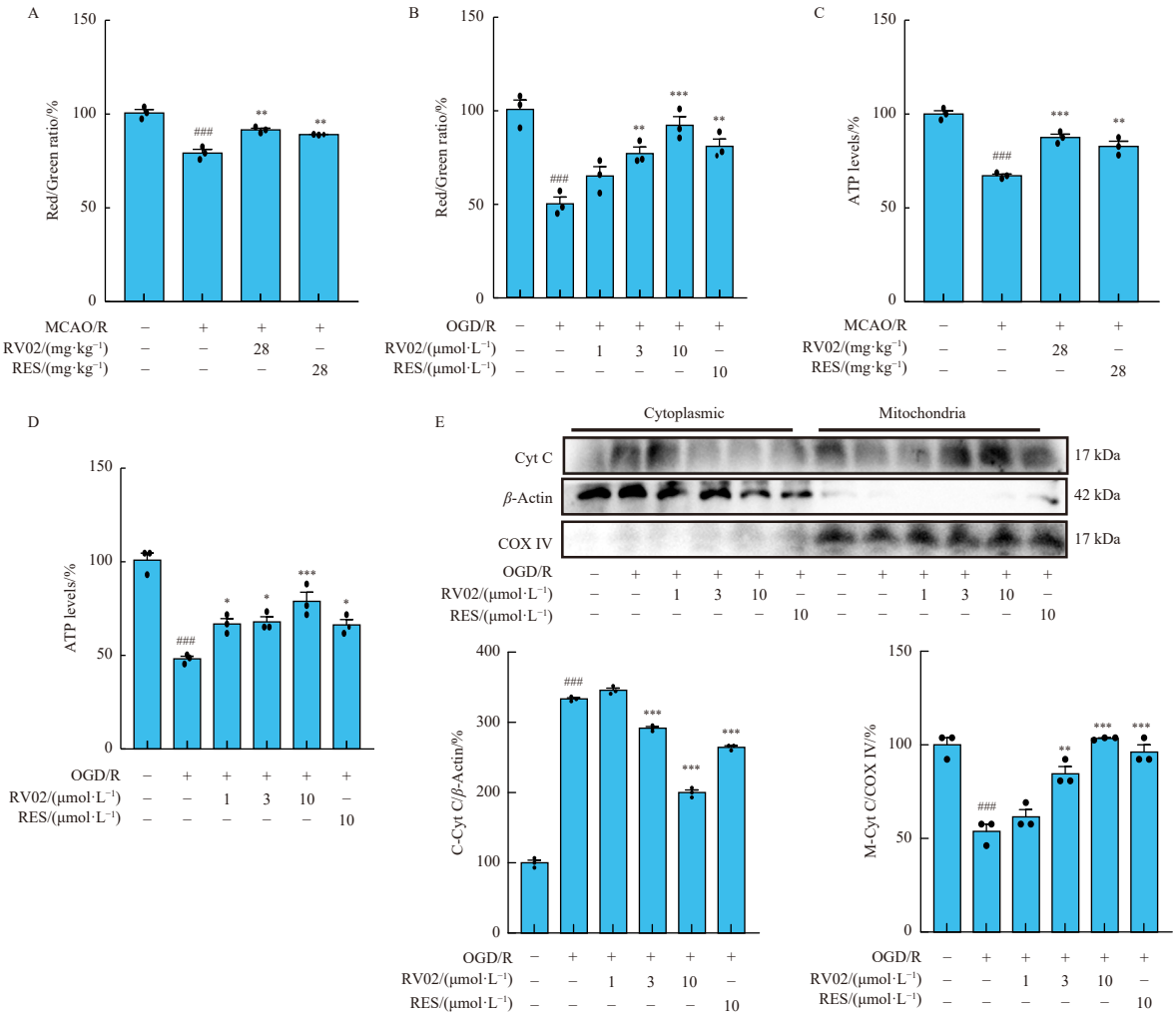

Fig. 4 RV02 ameliorates mitochondrial dysfunction induced by ischemia-reperfusion. (A and B) The alteration of MMPs was assessed *via* JC-1 staining in the cerebral cortex of MCAO/R rats or OGD/R-treated SH-SY5Y cells (n = 3). (C and D) The content of ATP in the cerebral cortex of MCAO/R rats or OGD/R-treated SH-SY5Y cells (n = 3). (E and F) The expression of mitochondrial Cyt C and cytoplasmic Cyt C in SH-SY5Y cells after OGD/R treatment (n = 3). Data are expressed as mean ± SEM. Statistics: one-way ANOVA followed by Tukey's test. $^{###}P < 0.001$ *vs* control; $^{*}P < 0.05$, $^{**}P < 0.01$, $^{***}P < 0.001$ *vs* MCAO/R group or OGD/R group. RES: resveratrol (28 mg·kg^{-1}, 10 μmol·L^{-1}).

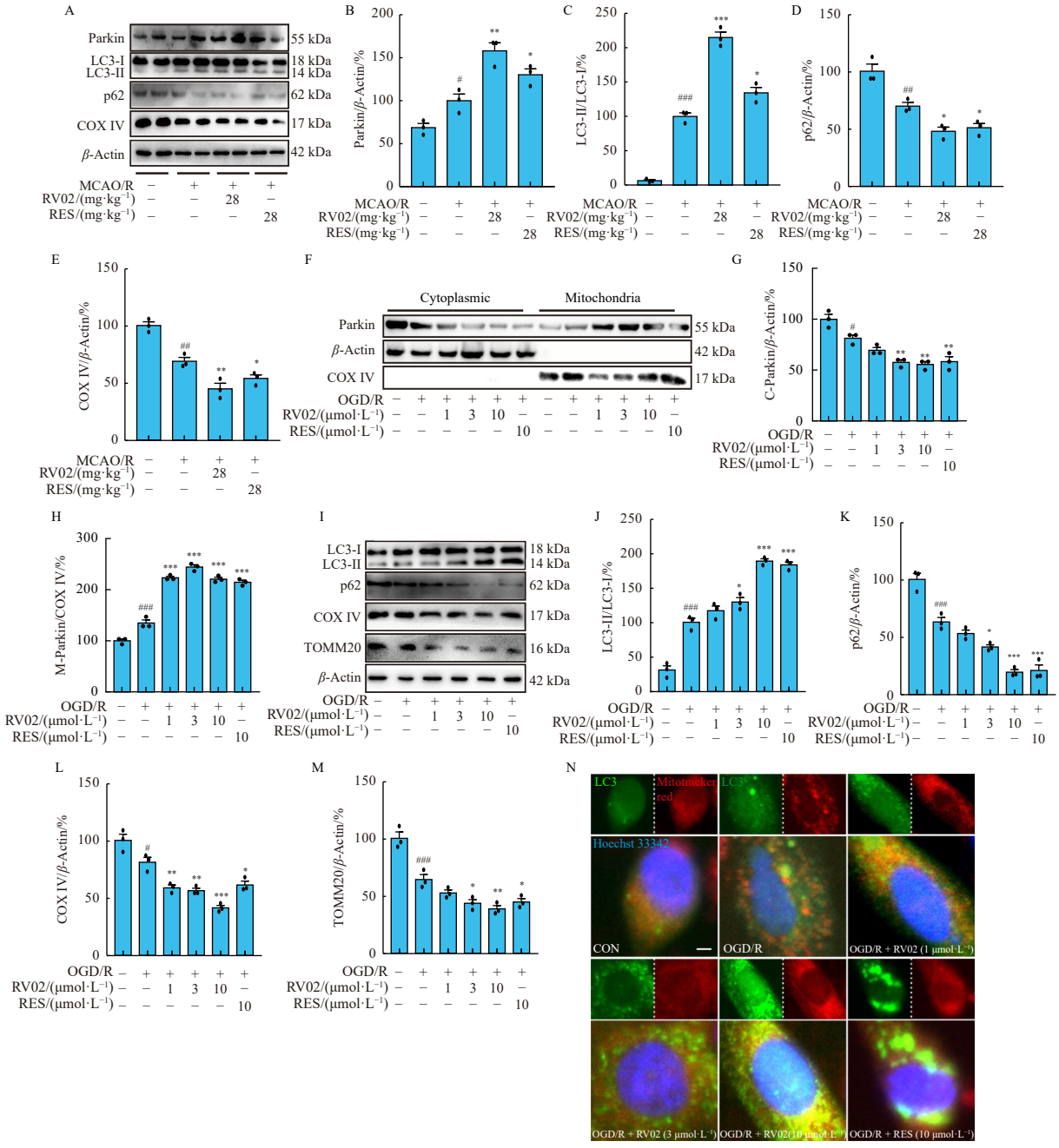

Fig. 5 RV02 enhanced mitophagy following ischemia/reperfusion. (A–E) Immunoblotting analysis of Parkin, LC3-II/LC3-I, p62, and COX IV expression in the cerebral cortex of MCAO/R rats (n = 3). (F–H) Immunoblotting analysis of cytoplasmic and mitochondrial Parkin expression in SH-SY5Y cells after OGD/R treatment (n = 3). (I–M) Immunoblotting analysis of LC3-II/LC3-I, p62, TOMM20, and COX IV expression in SH-SY5Y cells after OGD/R treatment (n = 3). (N) Co-localization of LC3-GFP and Mitotracker-Red in SH-SY5Y cells after OGD/R treatment (n = 3, scale bar: 20 μm). Data are presented as mean ± SEM. Statistical analysis: one-way ANOVA followed by Tukey's test. $^{\#}P$ <0.05, $^{\#\#}P$ < 0.01, $^{\#\#\#}P$ < 0.001 *vs* control; $^{*}P$ < 0.05, $^{**}P$ < 0.01, $^{***}P$ < 0.001 *vs* MCAO/R group or OGD/R group. RES: resveratrol (28 mg·kg^{-1}, 10 μmol·L^{-1}).

ive effect is associated with enhancing Parkin-mediated mitophagy, which facilitates the removal of damaged mitochondria and interrupts the cycle of mitochondrial damage and oxidative stress. These findings indicate the potential application of RV02 as a neuroprotective agent in clinical settings (Fig. 7).

Neurons in the brain are highly susceptible to damage from reduced blood flow, known as ischemic insult [41]. Limiting neuronal damage is crucial for the effective treatment of CIRI and improved stroke outcomes. This study indicates that RV02 can protect neurons and may be a promising therapeutic agent for stroke treatment. Strategies to reduce neuronal injury in stroke include regulating autophagy, inhibiting cell death pathways such as apoptosis and ferroptosis, and mitigating oxidative stress [29, 38, 42]. Neurons are particularly vulnerable to oxidative stress, which can lead to cell death and exacerbate brain damage after CIRI [29, 38]. Mitochondria play a critical role in energy production, ROS generation, and apoptotic signaling. Ischemia-reperfusion can induce mitochondrial damage, resulting in excessive ROS release, disruption of mitochondrial function, and ultimately cell death [13]. Previous research has demonstrated that the neuroprotective effects of RES are associated with enhanced mitochondrial function and reduced oxidative stress [43-45]. Our findings suggest that RV02's ability to ameliorate neuronal damage may be partially attributed to interrupting the cycle between mitochondrial damage and oxidative stress.

Mitophagy plays a pivotal role in regulating mitochondrial mass and ROS levels, encompassing both Parkin-dependent and non-dependent pathways. The Parkin-dependent mitophagy pathway has been the subject of extensive research. Following post-ischemic reperfusion, a typical increase in ROS levels occurs,

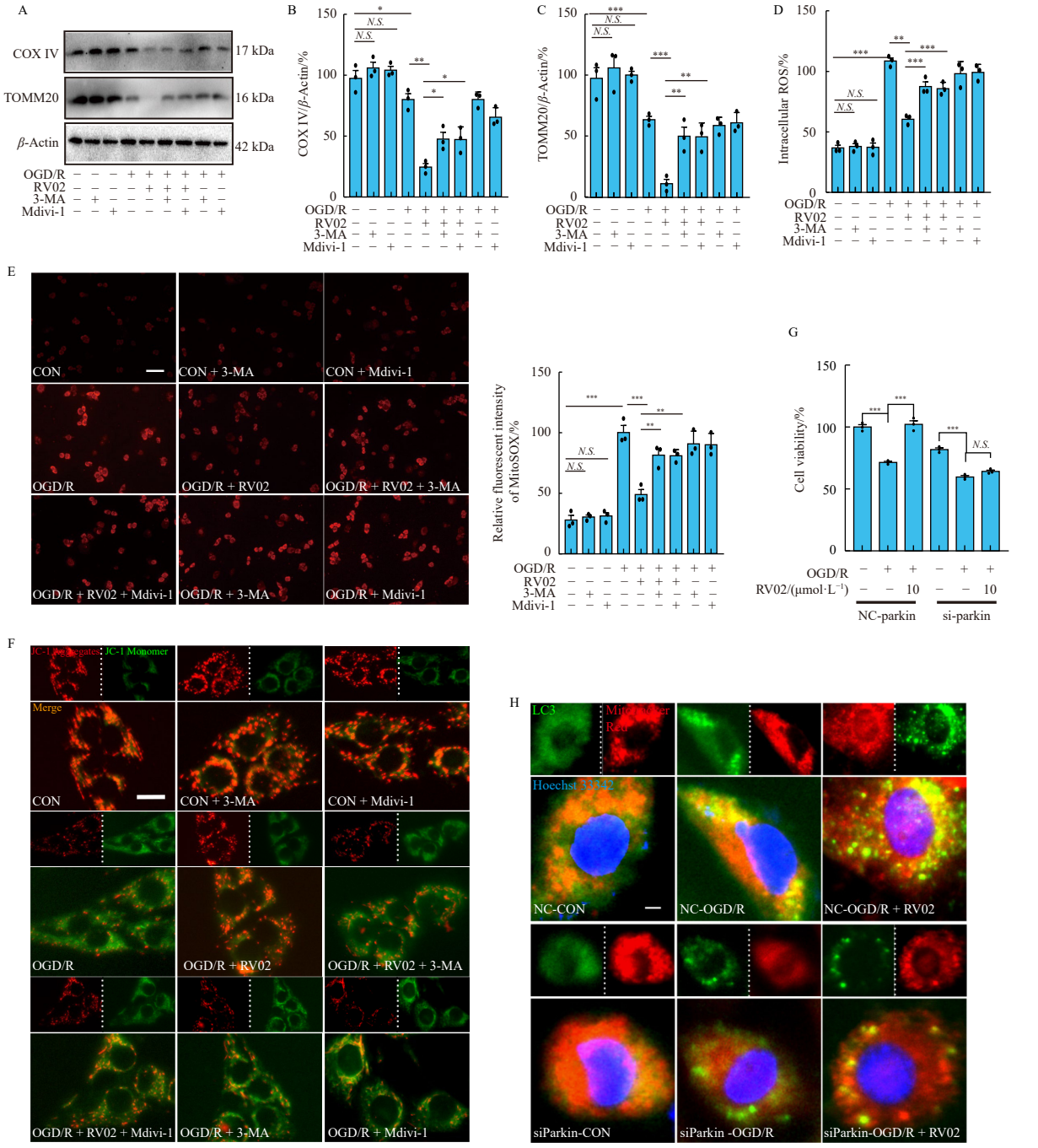

Fig. 6 RV02 mitigates mitochondrial damage and oxidative stress by enhancing Parkin-mediated mitophagy following ischemia/reperfusion. (A–C) COX IV and TOMM20 levels in SH-SY5Y cells subjected to OGD/R and subsequently treated with mitophagy inhibitor (Mdivi-1: 25 μmol·L $^{-1}$) or autophagy inhibitor (3-MA: 1 mmol·L $^{-1}$) (n = 3). (D) Intracellular ROS levels in SH-SY5Y cells exposed to OGD/R and then treated with mitophagy inhibitor (Mdivi-1: 25 μmol·L^{-1}) or autophagy inhibitor (3-MA: 1 mmol·L^{-1}) (n = 3), measured using DCFH-DA probe. (E) Mitochondrial ROS levels in SH-SY5Y cells subjected to OGD/R and subsequently treated with mitophagy inhibitor (Mdivi-1: 25 μmol·L $^{-1}$) or autophagy inhibitor (3-MA: 1 mmol·L $^{-1}$) (n = 3), detected using MitoSOX. Scale bar = 100 μm. (F) MMP imaging in SH-SY5Y cells exposed to OGD/R and then treated with mitophagy inhibitor (Mdivi-1: 25 μmol·L^{-1}) or autophagy inhibitor (3-MA: 1 mmol·L^{-1}) (n = 3), visualized using JC-1. Scale bar = 50 μm. (G) SH-SY5Y cell viability following treatment with NC-siRNA or si-Parkin and subsequent OGD/R exposure (n = 3). (H) Co-localization of LC3-GFP and Mitotracker-Red in SH-SY5Y cells after Parkin knockdown and OGD/R. Scale bar = 20 μm. Data are presented as mean ± SEM. Statistical analysis: one-way ANOVA followed by Tukey's test and independent sample t-test. $^{*}P < 0.05$, $^{**}P < 0.01$, $^{***}P < 0.001$ *vs* specified group.

disrupting mitochondrial membrane potential. This disruption leads to the translocation of Parkin from the cytoplasm to damaged mitochondria, thereby facilitating mitophagy. Research has shown that targeted modulation of mitophagy can serve as a neuroprotective strategy to mitigate ischemia-reperfusion injury [46, 47]. Our findings support the hypothesis that RV02 can alleviate cerebral ischemia-reperfusion injury through the modulation of mitophagy. However, it is crucial to note that RV02 not only regulates mitophagy but also influences apoptosis. Further studies are necessary to elucidate the mechanisms by which RV02 regulates apoptosis and promotes controlled mitophagy.

The regulation of Parkin-dependent mitophagy is considered a potential therapeutic strategy. Parkin-dependent mitophagy remains one of the most extensively studied mitophagy pathways. However, Parkin-independent mitophagy still involves several unknown mechanisms [48-51]. Research has demonstrated that BNIP3L-dependent mitophagy and Parkin-dependent mitophagy coexist in a complementary manner while also emphasizing the crucial role of Parkin-dependent mitophagy in ischemic stroke [52]. Moreover, precise control of Parkin levels is essential for mitochondrial biogenesis. Studies have shown that Parkin can enhance mitochondrial biogenesis and regulate ROS levels by ubi-

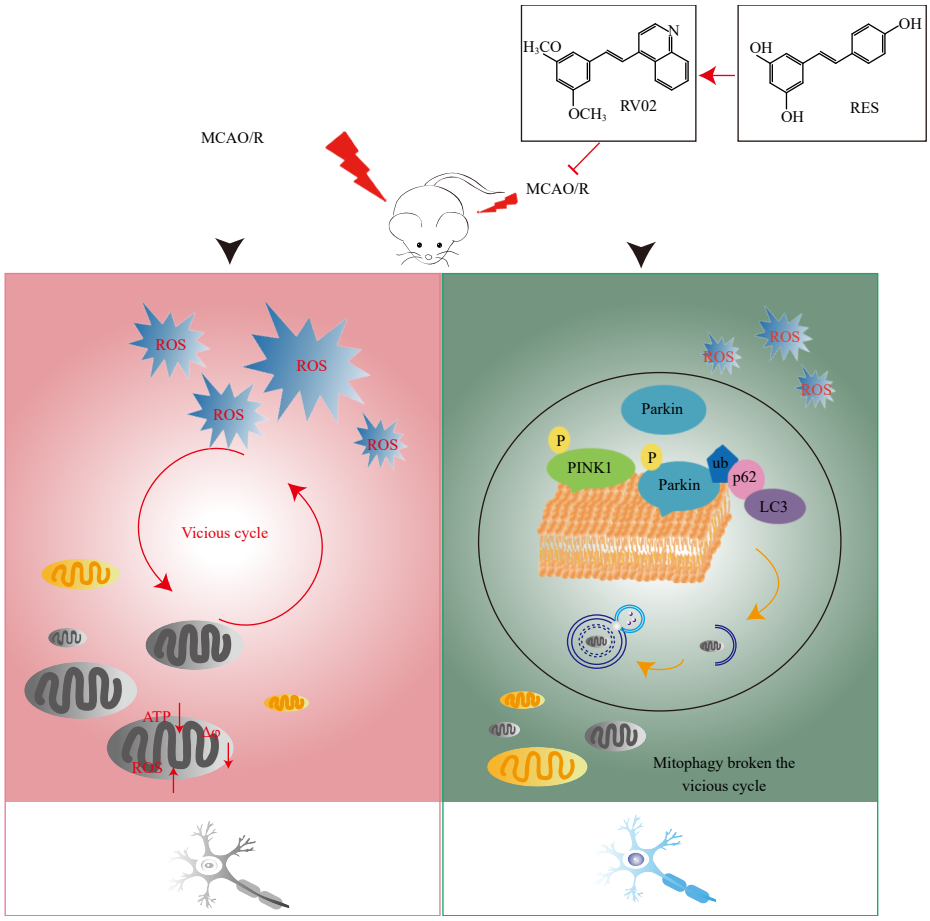

Fig. 7 Ischemia/reperfusion induces significant ROS accumulation and mitochondrial dysfunction, establishing a detrimental cycle between these two processes. RV02 disrupts this cycle by enhancing Parkin-mediated mitochondrial autophagy, thereby mitigating neuronal injury.

quitinating the Parkin-interacting protein PARIS, a transcriptional repressor of peroxisome proliferator-activated receptor gamma coactivator 1-alpha (PGC-1α) and coactivator of transcription factors such as nuclear respiratory factor 1 (NRF1) and nuclear factor erythroid 2-related factor 2 (NRF2) [53-55]. Parkin knockout has been associated with dopamine neuron degeneration and inhibition of neuronal development in mice [56, 57], underscoring Parkin's critical role in neuroprotection. Research has indicated that the neuroprotective effect of RES on neurons against OGD/R injury is linked to the promotion of Parkin-mediated mitophagy [58]. Our study demonstrated that RV02, a structural analog of RES, also regulates mitophagy and exerts neuroprotective effects by modulating Parkin. Previous research has shown RES regulation of Parkin transcription; further investigation is needed to determine if RV02 similarly influences Parkin transcription. Our findings also suggest that RV02 enhances autophagy flux, but the specific mechanism by which RV02 regulates this process requires further exploration.

5. Conclusions

In conclusion, this study demonstrates that RV02, a quinolinyl analog of RES, mitigates CIRI. The proposed mechanism involves the promotion of Parkin-mediated mitophagy, which prevents neuronal cell death by eliminating damaged mitochondria and reducing excessive accumulation of ROS in IS. Consequently, RV02 emerges as a promising therapeutic candidate for the treatment of IS.

Funding

This work was supported by the National Natural Science Foundation of China (No. 82174076), the Construction Project of Liaoning Provincial Key Laboratory, China (No. 2022JH13/10200026), the Fundamental Research Funds for the Central Universities (No. N2220002), the 111 Project (No. B16009), and the Research Project of Educational Commission of Liaoning Province (No. LJ212410164003).

Declaration of competing interest

These authors have no conflict of interest to declare.

References

1 Campbell BCV, Khatri P. Stroke. *Lancet*. 2020;396(10244):129-142. https://doi.org/10.1016/S0140-6736(20)31179-X.
2 Hankey GJ. Stroke. *Lancet*. 2017;389(10069):641-654. https://doi.org/10.1016/S0140-6736(16)30962-X.
3 Wu S, Wu B, Liu M, et al. Stroke in China: advances and challenges in epidemiology, prevention, and management. *Lancet Neurol*. 2019;18(4):394-405. https://doi.org/10.1016/S1474-4422(18)30500-3.
4 Zhao W, Zhang J, Sadowsky MG, et al. Remote ischaemic conditioning for preventing and treating ischaemic stroke. *Cochrane Database Syst Rev*. 2018;7(7):CD012503. https://doi.org/10.1002/14651858.CD012503.pub2.
5 Pirinen J, Järvinen V, Martinez-Majander N, et al. Left atrial dynamics is altered in young adults with cryptogenic ischemic stroke: a case-control study utilizing advanced echocardiography. *J Am Heart Assoc*. 2020;9(7):e014578. https://doi.org/10.1161/JAHA.119.014578.
6 Chen HS, Cui Y, Li XQ, et al. Effect of remote ischemic conditioning vs usual care on neurologic function in patients with acute moderate ischemic stroke: the RICAMIS randomized clinical trial. *JAMA*. 2022;328(7):627-636. https://doi.org/10.1001/jama.2022.13123.
7 Cai Y, Yang E, Yao X, et al. FUNDC1-dependent mitophagy induced by tPA protects neurons against cerebral ischemia-reperfusion injury. *Redox Biol*. 2021;38:101792. https://doi.org/10.1016/j.redox.2020.101792.
8 Shi K, Zou M, Jia DM, et al. tPA mobilizes immune cells that exacerbate hemorrhagic transformation in stroke. *Circ Res*. 2021;128(1):62-75. https://doi.org/10.1161/CIRCRESAHA.120.317596.
9 Savitz SI, Baron JC, Yenari MA, et al. Reconsidering neuroprotection in the reperfusion Era. *Stroke*. 2017;48(12):3413-3419. https://doi.org/10.1161/STROKEAHA.117.017283.
10 Tao T, Liu M, Chen M, et al. Natural medicine in neuroprotection for ischemic

stroke: challenges and prospective. *Pharmacol Ther*. 2020;216:107695. https://doi.org/10.1016/j.pharmthera.2020.107695.
11 Lai Y, Lin P, Chen M, et al. Restoration of L-OPA1 alleviates acute ischemic stroke injury in rats *via* inhibiting neuronal apoptosis and preserving mitochondrial function. *Redox Biol*. 2020;34:101503. https://doi.org/10.1016/j.redox.2020.101503.
12 Intihar TA, Martinez EA, Gomez-Pastor R. Mitochondrial dysfunction in Huntington's disease; interplay between HSF1, p53 and PGC-1α transcription factors. *Front Cell Neurosci*. 2019;13:103. https://doi.org/10.3389/fncel.2019.00103.
13 Guan R, Zou W, Dai X, et al. Mitophagy, a potential therapeutic target for stroke. *J Biomed Sci*. 2018;25(1):87. https://doi.org/10.1186/s12929-018-0487-4.
14 Teixeira J, Basit F, Swarts HG, et al. Extracellular acidification induces ROS- and mPTP-mediated death in HEK293 cells. *Redox Biol*. 2018;15:394-404. https://doi.org/10.1016/j.redox.2017.12.018.
15 Seidlmayer LK, Juettner VV, Kettlewell S, et al. Distinct mPTP activation mechanisms in ischaemia-reperfusion: contributions of Ca^{2+}, ROS, pH, and inorganic polyphosphate. *Cardiovasc Res*. 2015;106(2):237-248. https://doi.org/10.1093/cvr/cvv097.
16 Song X, Zhang L, Hui X, et al. Selenium-containing protein from selenium-enriched *Spirulina platensis* antagonizes oxygen glucose deprivation-induced neurotoxicity by inhibiting ROS-mediated oxidative damage through regulating MPTP opening. *Pharm Biol*. 2021;59(1):629-638. https://doi.org/10.1080/13880209.2021.1928715.
17 Zhang L, Dong Y, Wang W, et al. Ethionine suppresses mitochondria autophagy and induces apoptosis *via* activation of reactive oxygen species in neural tube defects. *Front Neurol*. 2020;11:242. https://doi.org/10.3389/fneur.2020.00242.
18 Thangaraj A, Periyasamy P, Guo ML, et al. Mitigation of cocaine-mediated mitochondrial damage, defective mitophagy and microglial activation by superoxide dismutase mimetics. *Autophagy*. 2020;16(2):289-312. https://doi.org/10.1080/15548627.2019.1607686.
19 Durcan TM, Fon EA. The three 'P's of mitophagy: PARKIN, PINK1, and post-translational modifications. *Genes Dev*. 2015;29(10):989-999. https://doi.org/10.1101/gad.262758.115.
20 Yu W, Sun Y, Guo S, et al. The PINK1/Parkin pathway regulates mitochondrial dynamics and function in mammalian hippocampal and dopaminergic neurons. *Hum Mol Genet*. 2011;20(16):3227-3240. https://doi.org/10.1093/hmg/ddr235.
21 Helton TD, Otsuka T, Lee MC, et al. Pruning and loss of excitatory synapses by the parkin ubiquitin ligase. *Proc Natl Acad Sci U S A*. 2008;105(49):19492-19497. https://doi.org/10.1073/pnas.0802280105.
22 Breuss JM, Atanasov AG, Uhrin P. Resveratrol and its effects on the vascular system. *Int J Mol Sci*. 2019;20(7):1523. https://doi.org/10.3390/ijms20071523.
23 Rauf A, Imran M, Butt MS, et al. Resveratrol as an anti-cancer agent: a review. *Crit Rev Food Sci Nutr*. 2018;58(9):1428-1447. https://doi.org/10.1080/10408398.2016.1263597.
24 Griñán-Ferré C, Bellver-Sanchis A, Izquierdo V, et al. The pleiotropic neuroprotective effects of resveratrol in cognitive decline and Alzheimer's disease pathology: from antioxidant to epigenetic therapy. *Ageing Res Rev*. 2021;67:101271. https://doi.org/10.1016/j.arr.2021.101271.
25 Walle T. Bioavailability of resveratrol. *Ann N Y Acad Sci*. 2011;1215:9-15. https://doi.org/10.1111/j.1749-6632.2010.05842.x.
26 Lin HS, Ho PC. A rapid HPLC method for the quantification of 3,5,4'-trimethoxy-trans-stilbene (TMS) in rat plasma and its application in pharmacokinetic study. *J Pharm Biomed Ana*. 2009; 49(2):387-392. https://doi.org/10.1016/j.jpba.2008.10.042.
27 Chiang YC, Wu YS, Kang YF, et al. 3,5,2',4'-Tetramethoxystilbene, a fully methylated resveratrol analog, prevents platelet aggregation and thrombus formation by targeting the protease-activated receptor 4 pathway. *Chem Biol Interact*. 2022;357:109889. https://doi.org/10.1016/j.cbi.2022.109889.
28 Yan Y, Yang J, Chen G, et al. Protection of resveratrol and its analogues against ethanol-induced oxidative DNA damage in human peripheral lymphocytes. *Mutat Res*. 2011;721(2):171-177. https://doi.org/10.1016/j.mrgentox.2011.01.012.
29 Chen H, He Y, Chen S, et al. Therapeutic targets of oxidative/nitrosative stress and neuroinflammation in ischemic stroke: applications for natural product efficacy with omics and systemic biology. *Pharmacol Res*. 2020;158:104877. https://doi.org/10.1016/j.phrs.2020.104877.
30 Xu L, Mi Y, Meng Q, *et al*. Anti-inflammatory effects of quinolinyl analog of resveratrol targeting TLR4 in MCAO/R ischemic stroke rat model. *Phytomedicine*. 2024;128:155344. https://doi.org/10.1016/j.phymed.2024.155344.
31 Chen G, Shan W, Wu Y, et al. Synthesis and anti-inflammatory activity of resveratrol analogs. *Chem Pharm Bull (Tokyo)*. 2005;53(12):1587-1590. https://doi.org/10.1248/cpb.53.1587.
32 Meng XL, Yang JY, Chen GL, et al. Effects of resveratrol and its derivatives on lipopolysaccharide-induced microglial activation and their structure-activity relationships. *Chem Biol Interact*. 2008;174(1):51-59. https://doi.org/10.1016/j.cbi.2008.04.015.
33 Mi Y, Jiao K, Xu JK, et al. Kellerin from *Ferula sinkiangensis* exerts neuroprotective effects after focal cerebral ischemia in rats by inhibiting microglia-mediated inflammatory responses. *J Ethnopharmacol*. 2021;269:113718. https://doi.org/10.1016/j.jep.2020.113718.
34 Hao T, Yang Y, Li N, et al. Inflammatory mechanism of cerebral ischemia-reperfusion injury with treatment of stepharine in rats. *Phytomedicine*. 2020;79:153353. https://doi.org/10.1016/j.phymed.2020.153353.
35 Longa EZ, Weinstein PR, Carlson S, et al. Reversible middle cerebral artery occlusion without craniectomy in rats. *Stroke*. 1989;20(1):84-91. https://doi.org/10.1161/01.STR.20.1.84.
36 Zou W, Song Y, Li Y, et al. The role of autophagy in the correlation between neuron damage and cognitive impairment in rat chronic cerebral hypoperfusion. *Mol Neurobiol*. 2018;55(1):776-791. https://doi.org/10.1007/s12035-016-0351-z.
37 Xu B, Qin Y, Li D, et al. Inhibition of PDE4 protects neurons against oxygen-glucose deprivation-induced endoplasmic reticulum stress through activation of the Nrf-2/HO-1 pathway. *Redox Biol*. 2020;28:101342. https://doi.org/10.1016/j.redox.2019.101342.
38 Xu P, Liu Q, Xie Y, et al. Breast cancer susceptibility protein 1 (BRCA1) rescues neurons from cerebral ischemia/reperfusion injury through NRF2-mediated antioxidant pathway. *Redox Biol*. 2018;18:158-172. https://doi.org/10.1016/j.redox.2018.06.012.
39 Cheng XT, Huang N, Sheng ZH. Programming axonal mitochondrial maintenance and bioenergetics in neurodegeneration and regeneration. *Neuron*. 2022;110(12):1899-1923. https://doi.org/10.1016/j.neuron.2022.03.015.
40 Lou G, Palikaras K, Lautrup S, et al. Mitophagy and neuroprotection. *Trends Mol Med*. 2020;26(1):8-20. https://doi.org/10.1016/j.molmed.2019.07.002.
41 Song X, Gong Z, Liu K, et al. Baicalin combats glutamate excitotoxicity *via* protecting glutamine synthetase from ROS-induced 20S proteasomal degradation. *Redox Biol*. 2020;34:101559. https://doi.org/10.1016/j.redox.2020.101559.
42 Fricker M, Tolkovsky AM, Borutaite V, et al. Neuronal cell death. *Physiol Rev*. 2018;98(2):813-880. https://doi.org/10.1152/physrev.00011.2017.
43 Yao Y, Zhou R, Bai R, et al. Resveratrol promotes the survival and neuronal differentiation of hypoxia-conditioned neuronal progenitor cells in rats with cerebral ischemia. *Front Med*. 2021;15(3):472-485. https://doi.org/10.1007/s11684-021-0832-y.
44 Xie YK, Zhou X, Yuan HT, et al. Resveratrol reduces brain injury after subarachnoid hemorrhage by inhibiting oxidative stress and endoplasmic reticulum stress. *Neural Regen Res*. 2019;14(10):1734-1742. https://doi.org/10.4103/1673-5374.257529.
45 Huang Y, Zhu X, Chen K, et al. Resveratrol prevents sarcopenic obesity by reversing mitochondrial dysfunction and oxidative stress *via* the PKA/LKB1/AMPK pathway. *Aging (Albany NY)*. 2019;11(8):2217-2240. https://doi.org/10.18632/aging.101910.
46 Shen Z, Zheng Y, Wu J, et al. PARK2-dependent mitophagy induced by acidic postconditioning protects against focal cerebral ischemia and extends the reperfusion window. *Autophagy*. 2017;13(3):473-485. https://doi.org/10.1080/15548627.2016.1274596.
47 Mao Z, Tian L, Liu J, et al. Ligustilide ameliorates hippocampal neuronal injury after cerebral ischemia reperfusion through activating PINK1/Parkin-dependent mitophagy. *Phytomedicine*. 2022;101:154111. https://doi.org/10.1016/j.phymed.2022.154111.
48 Li J, Yang D, Li Z, et al. PINK1/Parkin-mediated mitophagy in neurodegenerative diseases. *Ageing Res Rev*. 2023;84:101817. https://doi.org/10.1016/j.arr.2022.101817.
49 Zhang T, Xue L, Li L, *et al*. BNIP3 protein suppresses PINK1 kinase proteolytic cleavage to promote mitophagy. *J Biol Chem*. 2016;291(41):21616-21629. https://doi.org/10.1074/jbc.M116.733410.
50 Gao F, Chen D, Si J, et al. The mitochondrial protein BNIP3L is the substrate of PARK2 and mediates mitophagy in PINK1/PARK2 pathway. *Hum Mol Genet*. 2015;24(9):2528-2538. https://doi.org/10.1093/hmg/ddv017.
51 Ding WX, Ni HM, Li M, et al. Nix is critical to two distinct phases of mitophagy, reactive oxygen species-mediated autophagy induction and Parkin-ubiquitin-p62-mediated mitochondrial priming. *J Biol Chem*. 2010;285(36):27879-27890. https://doi.org/10.1074/jbc.M110.119537.
52 Yuan Y, Zheng Y, Zhang X, et al. BNIP3L/NIX-mediated mitophagy protects against ischemic brain injury independent of PARK2. *Autophagy*. 2017;13(10):1754-1766. https://doi.org/10.1080/15548627.2017.1357792.
53 Chung E, Choi Y, Park J, et al. Intracellular delivery of Parkin rescues neurons from accumulation of damaged mitochondria and pathological *α*-synuclein. *Sci Adv*. 2020;6(18):eaba1193. https://doi.org/10.1126/sciadv.aba1193.
54 Shin JH, Ko HS, Kang H, et al. PARIS (ZNF746) repression of PGC-1α contributes to neurodegeneration in Parkinson's disease. *Cell*. 2011;144(5):689-702. https://doi.org/10.1016/j.cell.2011.02.010.
55 Lee Y, Stevens DA, Kang SU, et al. PINK1 primes Parkin-mediated ubiquitination of PARIS in dopaminergic neuronal survival. *Cell Rep*. 2017;18(4):918-932. https://doi.org/10.1016/j.celrep.2016.12.090.
56 Jo A, Lee Y, Kam TI, et al. PARIS farnesylation prevents neurodegeneration in models of Parkinson's disease. *Sci Transl Med*. 2021;13(604):eaax8891. https://doi.org/10.1126/scitranslmed.aax8891.
57 Park MH, Lee HJ, Lee HL, et al. Parkin knockout inhibits neuronal development *via* regulation of proteasomal degradation of p21. *Theranostics*. 2017;7(7):2033-2045. https://doi.org/10.7150/thno.19824.
58 Ye M, Wu H, Li S. Resveratrol alleviates oxygen/glucose deprivation/reoxygenation-induced neuronal damage through induction of mitophagy. *Mol Med Rep*. 2021;23(1):73. https://doi.org/10.3892/mmr.2020.11711.